

We are IntechOpen, the world's leading publisher of Open Access books Built by scientists, for scientists

4,800

Open access books available

122,000

International authors and editors

135M

Downloads

Our authors are among the

154

Countries delivered to

TOP 1%

most cited scientists

12.2%

Contributors from top 500 universities



WEB OF SCIENCE™

Selection of our books indexed in the Book Citation Index
in Web of Science™ Core Collection (BKCI)

Interested in publishing with us?
Contact book.department@intechopen.com

Numbers displayed above are based on latest data collected.

For more information visit www.intechopen.com



Past, Present and Future of Finite Element Analysis in Dentistry

Ching-Chang Ko^{1,2,*}, Eduardo Passos Rocha^{1,3} and Matt Larson¹

¹*Department of Orthodontics,*

University of North Carolina School of Dentistry,

²*Department of Material Sciences and Engineering,*

North Carolina State University Engineering School, Raleigh,

³*Faculty of Dentistry of Araçatuba, UNESP,*

Department of Dental Materials and Prosthodontics, Araçatuba, São Paulo,

^{1,2}USA

³Brazil

1. Introduction

Biomechanics is fundamental to any dental practice, including dental restorations, movement of misaligned teeth, implant design, dental trauma, surgical removal of impacted teeth, and craniofacial growth modification. Following functional load, stresses and strains are created inside the biological structures. Stress at any point in the construction is critical and governs failure of the prostheses, remodeling of bone, and type of tooth movement. However, *in vivo* methods that directly measure internal stresses without altering the tissues do not currently exist. The advances in computer modeling techniques provide another option to realistically estimate stress distribution. Finite element analysis (FEA), a computer simulation technique, was introduced in the 1950s using the mathematical matrix analysis of structures to continuum bodies (Zienkiewicz and Kelly 1982). Over the past 30 years, FEA has become widely used to predict the biomechanical performance of various medical devices and biological tissues due to the ease of assessing irregular-shaped objects composed of several different materials with mixed boundary conditions. Unlike other methods (e.g., strain gauge) which are limited to points on the surface, the finite element method (FEM) can quantify stresses and displacement throughout the anatomy of a three dimensional structure.

The FEM is a numerical approximation to solve partial differential equations (PDE) and integral equations (Hughes 1987, Segerlind 1984) that are formulated to describe physics of complex structures (like teeth and jaw joints). Weak formulations (virtual work principle) (Lanczos 1962) have been implemented in FEM to solve the PDE to provide stress-strain solutions at any location in the geometry. Visual display of solutions in graphic format adds attractive features to the method. In the first 30 years (1960-1990), the development of FEM

* Corresponding Author

programs focused on stability of the solution including minimization of numerical errors and improvement of computational speed. During the past 20 years, 3D technologies and non-linear solutions have evolved. These developments have directly affected automobile and aerospace evolutions, and gradually impacted bio-medicine. Built upon engineering achievement, dentistry shall take advantage of FEA approaches with emphasis on mechanotherapy. The following text will review history of dental FEA and validation of models, and show two examples.

2. History of dental FEA

2.1 1970-1990: Enlightenment stage -2D modeling

Since Farah's early work in restorative dentistry in 1973, the popularity of FEA has grown. Early dental models were two dimensional (2D) and often limited by the high number of calculations necessary to provide useful analysis (Farah and Craig 1975, Peters et al., 1983, Reinhardt et al., 1983, Thresher and Saito 1973). During 1980-1990, the plane-stress and plane-strain assumptions were typically used to construct 2D tooth models that did not contain the hoop structures of dentin because typically either pulp or restorative material occupied the central axis of the tooth (Anusavice et al., 1980). Additional constraints (e.g., side plate and axisymmetric) were occasionally used to patch these physical deficiencies (hoop structures) to prevent the separation of dentin associated with the 2D models (Ko, 1989). As such a reasonable biomechanical prediction was derived to aid designs of the endodontic post (Ko et al., 1992). Axisymmetric models were also used to estimate stress distribution of the dental implants with various thread designs (Rieger et al., 1990). Validation of the FE models was important in this era because assumptions and constraints were added to overcome geometric discontinuity in the models, leading to potential mathematical errors.

2.2 "1990-2000" beginnings stage of 3D modeling

As advancements have been made in imaging technologies, 3D FEA was introduced to dentistry. Computer tomography (CT) data provide stacks of sectional geometries of human jaws that could be digitized and reconstructed into the 3D models. Manual and semi-automatic meshing was gradually evolved during this time. The 3D jaw models and tooth models with coarse meshes were analyzed to study chewing forces (Korioth 1992, Korioth and Versluis 1997, Jones et al., 2001) and designs of restorations (Lin et al., 2001). In general, the element size was relatively large due to the immature meshing techniques at that time, which made models time consuming to build. Validation was required to check accuracy of the stress-strain estimates associated with the coarse-meshed models. In addition to the detail of 3D reconstruction, specific solvers (e.g., poroelasticity, homogenization theory, dynamic response) were adapted from the engineering field to study dental problems that involved heterogeneous microstructures and time-dependent properties of tissues. Interfacial micromechanics and bone adaptation around implants were found to be highly non-uniform, which may dictate osseointegration patterns of dental implants (Hollister et al., 1993; Ko 1994). The Monte Carlo model (probability prediction), with incorporation of the finite element method for handling irregular tooth surface, was developed by Wang and

Ko et al (1999) to stimulate optical scattering of the incipient caries (e.g., white spot lesion). The simulated image of the lesion surface was consistent with the true image captured *in clinic* (Figure 1). Linear fit of the image brightness between the FE and clinical images was 85% matched, indicating the feasibility of using numerical model to interpret clinical white spot lesions. The similar probability method was recently used to predict healing bone adaptation in tibia (Byrne et al., 2011). Recognition of the importance of 3D models and specific solutions were the major contributions in this era.

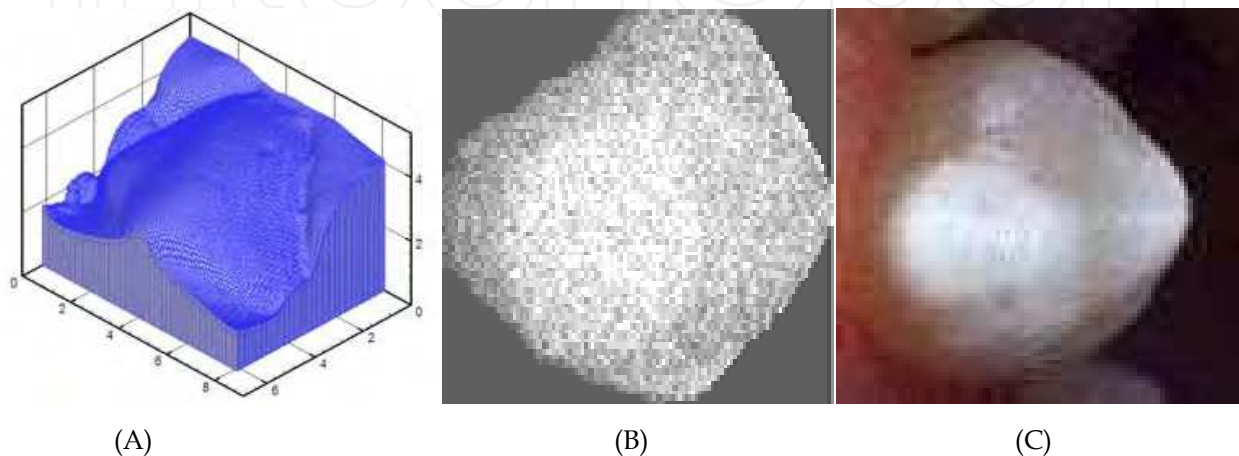


Fig. 1. **A.** Finite element mesh of *in vivo* carious tooth used for Monte Carlo simulation; **B.** Image rendered from Monte Carlo 3D simulation, **C.** True image of carious tooth obtained from a patient's premolar using an intra-oral camera.

2.3 “2000-2010” age of proliferation, 3D with CAD

As advancements have been made in computer and software capability, more complex 3D structures (e.g., occlusal surfaces, pulp, dentin, enamel) have been simulated in greater detail. Many recent FE studies have demonstrated accurate 3D anatomic structures of a sectioned jaw-teeth complex using μ CT images. Increased mathematical functions in 3D computer-aid-design (CAD) have allowed accurate rendition of dental anatomy and prosthetic components such as implant configuration and veneer crowns (Figure 2). Fine meshing and high CPU computing power appeared to allow calculation of mechanical fields (e.g., stress, strain, energy) accounting for anatomic details and hierarchy interfaces between different tissues (e.g., dentin, PDL, enamel) that were offered by the CAD program. It was also recognized that inclusion of complete dentition is necessary to accurately predict stress-strain fields for functional treatment and jaw function (Field et al. 2009). Simplified models containing only a single tooth overlooked the effect of tooth-tooth contacts that is important in specified biomechanical problems such as orthodontic tooth movement and traumatic tooth injury. CAD software such as SolidWorks© (Waltham, MA, USA), Pro Engineering© (Needham, MA), and Geomagic (Triangle Park, NC, USA) have been adapted to construct dentofacial compartments and prostheses. These CAD programs output solid models that are then converted to FE programs (e.g., Abaqus, Ansys, Marc, Mimics) for meshing and solving. The automeshing capability of FE programs significantly improved during this era.

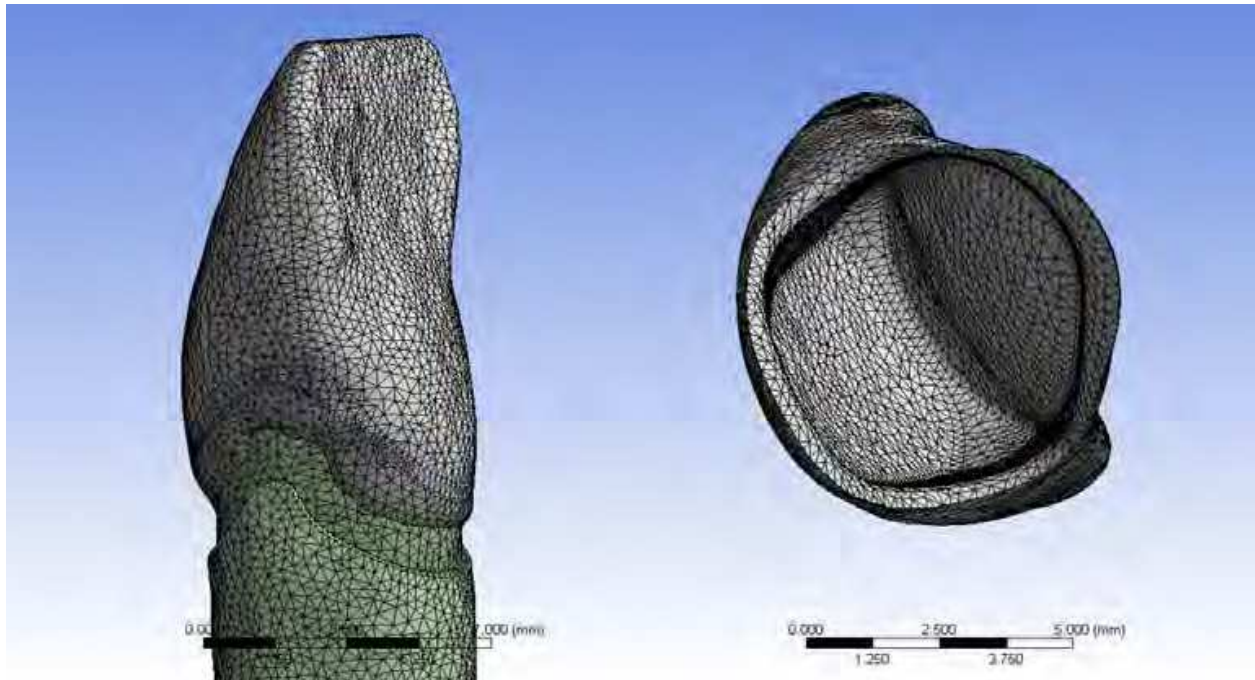


Fig. 2. Fine finite element mesh generated for ceramics veneer simulation.

3. Current development of 3D dental solid models using CAD programs

Currently, solid models have been created from datasets of computer tomography (CT) images, microCT images, or magnetic resonance images (MRI). To create a solid model from an imaging database, objects first need to be segregated by identifying interfaces. This is performed through the creation of non-manifold assemblies either through sequential 2D sliced or through segmentation of 3D objects. For this type of model reconstruction, the interfaces between different bodies are precisely specified, ensuring the existence of common nodes between different objects of the contact area. This provides a realistic simulation of load distribution within the object. For complex interactions, such as bone-implant interfaces or modeling the periodontal ligament (PDL), creation of these coincident nodes is essential.

When direct engineering (forward engineering) cannot be applied, reverse engineering is useful for converting stereolithographic (STL) objects into CAD objects (.iges). Despite minor loss of detail, this was the only option for creation of 3D organic CAD objects until the development of 3D segmentation tools and remains a common method even today. The creation of STL layer-by-layer objects requires segmentation tools, such as ITK-SNAP (Yushkevich et al., 2006) to segment structures in 3D medical images. SNAP provides semi-automatic segmentation using active contour methods, as well as manual delineation and image navigation.

Following segmentation, additional steps are required to prepare a model to be imported into CAD programs. FEA requires closed solid bodies - in other words, each part of the model should be able to hold water. Typical CT segmentations yield polygon surfaces with irregularities and possible holes. A program capable of manipulating these polygons and creating solid CAD bodies is required, such as Geomagic (Triangle Park, NC, USA).

Although segmentations may initially appear very accurate (Figure 3A), there are often many small irregularities that must be addressed (Figure 3B). Obviously, organic objects will have natural irregularities that may be important to model, but defects from the scanning and segmentation process must be removed. Automated processes in Geomagic such as mesh doctor can identify problematic areas (Figure 3B) and fix many minor problems. For larger defects, defeaturing may be required. Once the gaps in the surface have been filled, some amount of smoothing is typically beneficial. Excess surface detail that will not affect results only increases the file size, meshing times, mesh density, and solution times. To improve surfacing, a surface mesh on the order of 200,000 polygons is recommended. Geomagic has a tool ("optimize for surfacing") that redistributes the polygons nodes on the surface to create a more ideal distribution for surfacing (Figure 3C). Following these optimization steps, it is important to compare the final surface to the initial surface to verify that no significant changes were made.

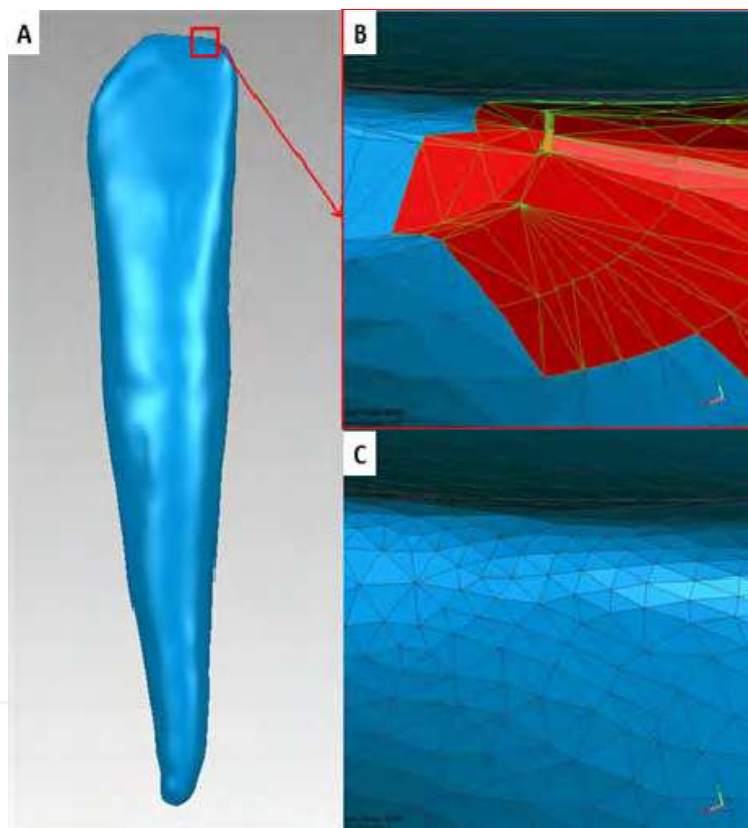


Fig. 3. Although initial geometry following segmentation can appear smooth (A), many small defects are present that Geomagic will highlight in red using "mesh doctor" as potentially problematic (B). Following closing gaps, smoothing, minor defeaturing, and optimization for surfacing, the polygon mesh is greatly improved (C).

With the optimized surfaces prepared using the previous steps, closed solid bodies can be created. Although the actual final bodies with the interior and exterior surfaces can be created at this stage, we have observed that closing each surface independently and using Booleans in the CAD program typically improves results. For example, this forces the interior surface of the enamel to be the identical surface as the exterior of the dentin. If the Boolean operations are done prior to surfacing, minor differences in creating NURB surfaces

may affect the connectivity of the objects. Some research labs (Bright and Rayfield 2011) will simply transfer the polygon surfaces over to a FEA program for analysis without using a CAD program. This can be very effective for relatively simple models, but when multiple solid bodies are included and various mesh densities are required this process becomes cumbersome.

To use a CAD program with organic structures, the surface cannot be a polygon mesh, but rather needs to have a mathematical approximation of the surface. This is typically done with NURB surfaces, so the solid can be saved as an .iges or .step file. This process involves multiple steps - laying out patches, creating grids within these patches, optimizing the surface detail, and finally creating the NURB surface (Figure 4). Surfacing must be done carefully as incorrectly laying out the patches on the surface or not allowing sufficient detail may severely distort the surface. In the end, the surfaced body should not have problematic geometry, such as sliver faces, small faces, or small edges.

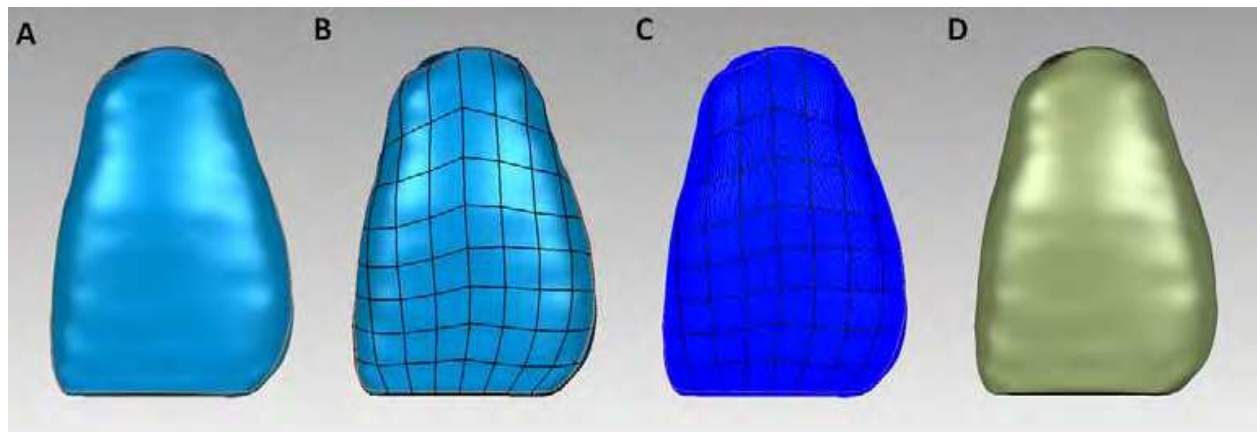


Fig. 4. Process of NURB surface generation using Geomagic. (A) Contour lines are defined that follow the natural geometry - in this case, line angles were used. (B) Patches are constructed and shuffled to create a clean grid pattern. (C) Grids are created within each patch. (D) NURB surfaces are created by placing control points along the created grids.

CAD programs allow the incorporation of high definition materials or parts from geometry files (e.g. .iges, .step), such as dentures, prosthesis, orthodontics appliances, dental restorative materials, surgical plates and dental implants. They even allow partial modification of the solid model obtained by CT or μ CT to more closely reproduce accurate organic geometry. Organic modeling (biomodeling) extensively uses splines and curves to model the complex geometry. FE software or other platforms with limited CAD tools typically do not provide the full range of features required to manipulate these complicated organic models. Therefore, the use of a genuine CAD program is typically preferred for detailed characterization of the material and its contact correlation with surrounding structures. This is especially true for models that demand strong modification of parts or incorporation of multiple different bodies.

When strong modification is required, the basic parts of the model such as bone, skin or basic structures can be obtained in .stl format. They are then converted to a CAD file allowing modification and/or incorporation of new parts before the FE analysis. It is also possible to use the CT or microCT dataset to directly create a solid in the CAD program.

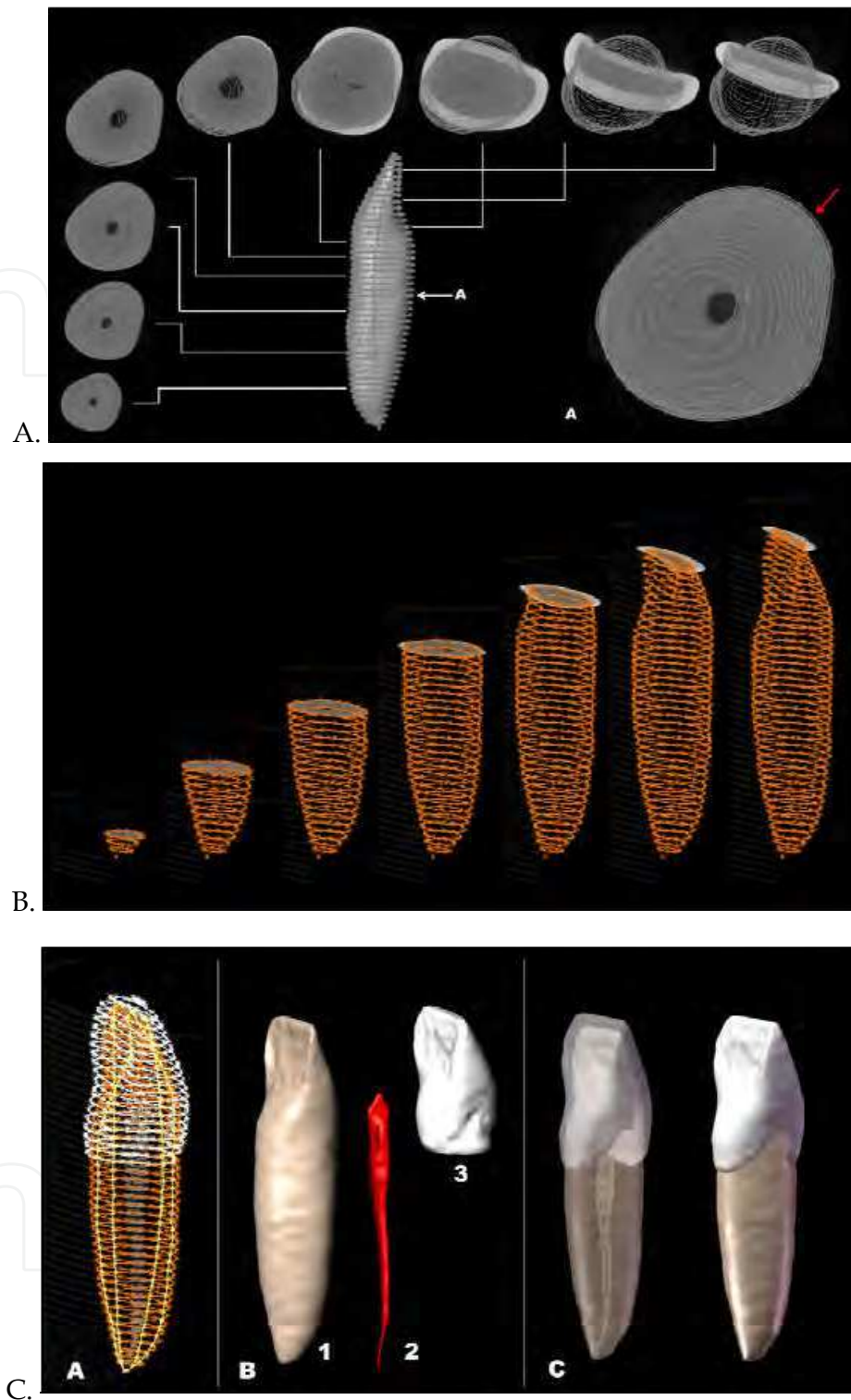


Fig. 5. The solid model of a maxillary central incisor was created through the following steps. (A) Multiple sketches were created in various slices of the microCT data. The sketch defined the contour of the root. (B) Sequential contours were used to reconstruct outer surface of dentin and other parts (e.g., enamel and pulp - not shown). (C) All parts (enamel, dentin and pulp) were combined to form the solid model of the central incisor. All procedures were performed using SolidWorks software.

Initially, this procedure might be time-consuming. However, it is useful for quickly and efficiently making changes in parts, resizing multiple parts that are already combined, and incorporating new parts. This also allows for serial reproduction of unaltered parts of the model, such as loading areas and unaltered support structures, keeping their dimensions and Cartesian coordinates.

This procedure involves the partial or full use of the dataset, serially organized, to create different parts. (Figures 5 A & B) In models with multiple parts, additional tools such as lofts, sweeps, surfaces, splines, reference planes, and lines can be used to modify existing solids or create new solids (Figures 5C). Different parts may be combined through Boolean operations to generate a larger part, to create spaces or voids, or to modify parts. The parts can be also copied, moved, or mirrored in order to reproduce different scenarios without creating an entirely new model.

4. Finite element analysis of the current dental models

4.1 Meshing

For discretization of the solid model, most FE software has automated mesh generating features that produce rather dense meshes. However, it is important to enhance the controller that configures the elements including types, dimensions, and relations to better fit the analysis to a particular case and its applications. Most of current FE software is capable of assessing the quality of the mesh according to element aspect ratio and the adaptive method. The ability of the adaptive method to automatically evaluate and modify the contact area between two objects overlapping the same region and to refine the mesh locally in areas of greater importance and complexity has profoundly improved the accuracy of the solution. Although automated mesh generation has greatly improved, note that it still requires careful oversight based on the specific analysis being performed. For example, when examining stresses produced in the periodontal ligament with orthodontic appliances, the mesh will be greatly refined in the small geometry of the orthodontic bracket, but may be too coarse in the periodontal ligament – the area of interest.

The validation that was concerned with meshing errors and morphological inaccuracy during 1970 – 2000 is no longer a major concern as the CAD and meshing technology evolves. However, numerical convergence (Huang et al., 2007) is still required, which is frequently neglected in dental simulations (Tanne et al., 1987; Jones et al., 2001; Liang et al., 2009; Kim et al., 2010). Some biologists ignore all results from FEA, requesting an unreasonable level of validation for each model, but overlooking the valuable contributions of engineering principles. A rational request should recognize evolution of the advanced technologies but focus on numerical convergence. The numerical convergence is governed by two factors, continuity and approximation methods, and can be classified to strong convergence $||X_n|| \rightarrow ||X||$ as $n \rightarrow \infty$ and weak convergence $\int(X_n) \rightarrow \int(X)$ as $n \rightarrow \infty$ where X_n represents physical valuables such as displacement, temperature, and velocity. X represents the exact solution and \int indicates the potential energy. It is recommended that all dental FE models should test meshing convergence prior to analyses.

4.2 Validity of the models

The validity of the dental FEA has been a concern for decades. Two review articles (Korioth and Versluis, 1997; Geng et al., 2001) in dentistry provided thorough discussions about effects of geometry, element type and size, material properties, and boundary conditions on the accuracy of solutions. In general these discussions echoed an earlier review by Huiskes and Cao (1983). The severity of these effects has decreased as the technologies and knowledge evolved in the field. In the present CAD-FEA era, the consideration of FEA accuracy in relation to loading, boundary (constraint) conditions, and validity of material properties are described as follows:

4.2.1 Loading

The static loading such as bite forces is usually applied as point forces to study prosthetic designs and dental restorations. The bite force, however, presents huge variations (both magnitude and direction) based on previous experimental measures (Proffit et al., 1983; Proffit and Field 1983). Fortunately, FEA allows for easy changes in force magnitudes and directions to approximate experimental data, which can serve as a reasonable parametric study to assess different loading effects. On the other hand, loading exerted by devices such as orthodontic wires is unknown or never measured experimentally, and should be simulated with caution (see the section 5.2)

4.2.2 Boundary Condition (BC)

The boundary condition is a constraint applied to the model, from which potential energy and solutions are derived. False solutions can be associated at the areas next to the constraints. As a result, most dental models set constraints far away from the areas of interest. Based on the Saint-Venant's principle, the effects of constraints at sufficiently large distances become negligible. However, some modeling applies specific constraints to study particular physical phenomenon. For example, the homogenization theory was derived to resolve microstructural effects in composite by applying periodic constraints (Ko et al., 1996). It was reported that using homogenization theory to estimate bone-implant interfacial stresses by accounting for microstructural effects might introduce up to 20% error (Ko 1994).

4.2.3 Material properties

Mechanical properties of biological tissues remain a major concern for the FE approach because of the viscoelastic nature of biological tissues that prevents full characterization of its time-dependent behaviors. Little technology is available to measure oral tissue properties. Most FE studies in dentistry use the linear elastic assumption. Data based on density from CT images can be used to assign heterogeneous properties. Few researches attempting to predict non-linear behaviors using bilinear elastic constants aroused risks for a biased result (Cattaneo et al., 2009). Laboratory tests excluding tissues (e.g., PDL) were also found to result in less accurate data than computer predictions (Chi et al., 2011). Caution must be used when laboratory data is applied to validate the model. To our knowledge, the most valuable data for validation resides on clinical assessments such as measuring tooth movement (Yoshida et al., 1998; Brosh et al., 2002).

4.3 Solution/principle

The weak form of the equilibrium equation for classic mechanics is given below:

$$\int_{\Omega^e} c_{ijkl} \varepsilon_{ij}(v) \varepsilon_{kl}(u) d\Omega^e = \int_{\Gamma} t_i v_i d\Gamma, \text{ where } \Omega^e \text{ represents the total domain of the object, and}$$

t_i represents tractions. ε is obtained by applying the small strain-displacement relationship

$$\varepsilon_{ij}(u) = \frac{1}{2} \left(\frac{\partial u_i}{\partial x_j} + \frac{\partial u_j}{\partial x_i} \right). \text{ Stresses will be obtained by the constitutive law } \sigma_{ij} = E_{ijkl} \varepsilon_{kl}. \text{ Using}$$

the variational formulation and mesh discretization, this equilibrium equation can be assembled by the individual element $\int_{\Omega^e} [B]^t [D] [B] d\Omega^e$. plus the boundary integral where B

is the shape function and D is element stiffness matrix. The element stiffness matrix represents material property of either a linear or non-linear function. As mentioned above, mechanical properties of oral tissues are poorly characterized. The most controversial oral tissue is the PDL due to its importance in supporting teeth and regulating alveolar bone remodeling. To date, studies conducted to characterize non-linear behaviors of the PDL are not yet conclusive. One approximation of PDL properties assumes zero stiffness under low compression resulting in very low stress under compression (Cattaneo et al., 2009). Interpretation of such non-linear models must be approached with cautious. Consequently, linear elastic constants are frequently used for dental simulations to investigate initial responses under static loading.

In addition to the commonly used point forces, the tractions (t_i) in dental simulations should consider preconditions (e.g., residual stress, polymerization shrinkage and unloading of orthodontic archwire). Previously, investigation of composite shrinkage yielded valuable contributions to restorative dentistry (Magne et al., 1999). In the following section, we will demonstrate two applications using submodels from a full dentition CAD model: one with static point loading and the other with deactivated orthodontic archwire bending.

5. Examples of dental FEA

As described in Section 3, a master CAD model with full dentition was developed. The model separates detailed anatomic structures such as PDL, pulp, dentin, enamel, lamina dura, cortical bone, and trabecular bone. This state-of-the-art model contains high order NURB surfaces that allow for fine meshing, with excellent connectivity so the model can be conformally meshed with concurrent nodes at all interfaces. Many submodels can be isolated from this master model to study specified biomechanical questions. Two examples presented here are the first series of applications: orthodontic miniscrews and orthodontic archwires for tooth movement.

5.1 Orthodontic miniscrews

5.1.1 Introduction

The placement of miniscrews has become common in orthodontic treatment to enhance tooth movement and to prevent unwanted anchorage loss. Unfortunately, the FE biomechanical miniscrew models reported to date have been oversimplified or show

incomplete reflections of normal human anatomy. The purpose of this study was to construct a more anatomically accurate FE model to evaluate miniscrew biomechanics. Variations of miniscrew insertion angulations and implant materials were analyzed.

5.1.2 Methods

A posterior segment was sectioned from the full maxillary model. Borders of the model were established as follows: the mesial boundary was at the interproximal region between the maxillary right canine and first premolar; the distal boundary used the distal aspect of the maxillary tuberosity; the inferior boundary was the coronal anatomy of all teeth; and the superior boundary was all maxillary structures (including sinus and zygoma) up to 15mm superior to tooth apices (Figure 6A).

An orthodontic miniscrew (TOMAS®, 8mm long, 1.6mm diameter) was created using Solidworks CAD software. The miniscrew outline was created using the Solidworks sketch function and revolved into three dimensions. The helical sweep function was used to create a continuous, spiral thread. Subtraction cuts were used to create the appropriate head configuration after hexagon ring placement. The miniscrew was inserted into the maxillary model from the buccal surface between the second premolar and first molar using Solidworks. The miniscrew was inserted sequentially at angles of 90°, 60° and 45° vertically relative to the surface of the cortical bone (Figure 6B), and was placed so that the miniscrew neck/thread interface was coincident with the external contour of the cortical bone. For each angulation, the point of intersection between the cortical bone surface and the central axis of the miniscrew was maintained constant to ensure consistency between models. Boolean operations were performed and a completed model assembly was created at each angulation.

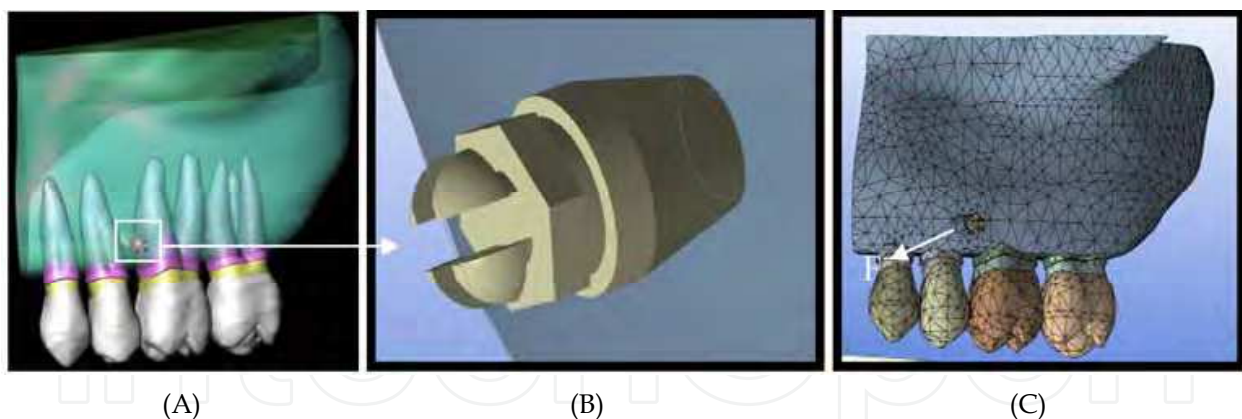


Fig. 6. The FE model of the orthodontic miniscrew used in the present study. (A) The solid model of four maxillary teeth plus the miniscrew was created using SolidWorks. (B) Close look of the miniscrew inserted to the bone. (C) FE mesh was generated by Ansys Workbench 10.0. F indicates the force ($1.47\text{ N} = 150\text{ gm}$) applied to the miniscrew.

The IGES format file of each finished 3D model was exported to ANSYS 10.0 Workbench (Swanson Analysis Inc., Huston, PA, USA), and FE models with 10-node tetrahedral elements were generated for each assembly. The final FE mesh generated for each model contained approximately 91,500 elements, which was sufficient to obtain solution convergence. Following FE mesh generation, the model was fixed at the palatal, mesial, and

superior boundaries. A 150 grams loading force to the mesial was then applied to the miniscrew to simulate distalization of anterior teeth (Figure 6C). All materials were linear and isotropic (Table 1), and the miniscrew/bone interface was assumed to be rigidly bonded. Three material properties (stainless steel, titanium, and composite) were used for the miniscrew. Each model was solved under the small displacement assumption. Two-way ANOVA was used to compare effects of angulation and material.

	Cortical	Trabecular	PDL	Dentin	Enamel	Pulp	Stainless Steel (SS)	Titanium (Ti)	Composite
Young's Modulus (MPa)	13,700	1370	175	18,000	77,900	175	190,000	113,000	20,000
Poisson's Ratio	0.3	0.3	0.4	0.3	0.3	0.4	0.3	0.3	0.3

Table 1. Computer model component material properties (O'Brien, 1997)

5.1.3 Results

Angle effect

Stress patterns in both cortical bone and the miniscrew from each simulation were concentrated in the second premolar/first molar area immediately around the implant/bone interface (Figure 7). Peak stress values for each model simulation are listed in Table 2. Peak maximum principal stress (MaxPS) within the miniscrew was greatest when angle placement was 45°. Peak MaxPS was lowest at the 60° placement angle. Peak MaxPS in cortical bone was greatest at 45° angulation, except for the stainless steel implant. In each angulation, the location of greatest maximum principle stress was located at the distal aspect of the miniscrew/cortical bone interface. Similarly, peak minimum principal stress (MinPS) was lowest on the miniscrew at 60° and greatest at 45°. Figure 8 shows mean stress plots for all angulations and materials. Angulation difference was statistically significant for miniscrews at 45° compared to 60° and 90° for all stress types analyzed (MaxPS $p=0.01$, MinPS $p=0.01$, von Mises stress (vonMS) $p=0.01$). There is no significant difference in cortical bone stress at any angulation.

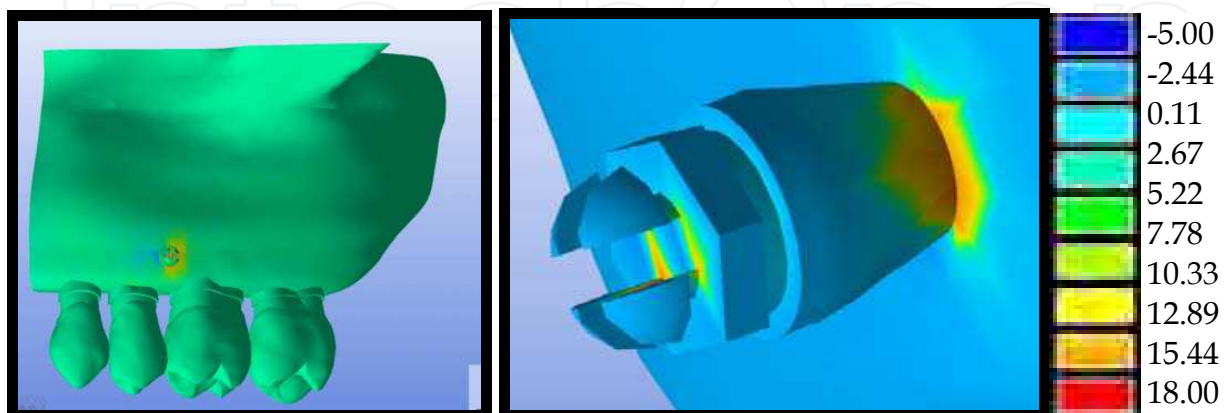
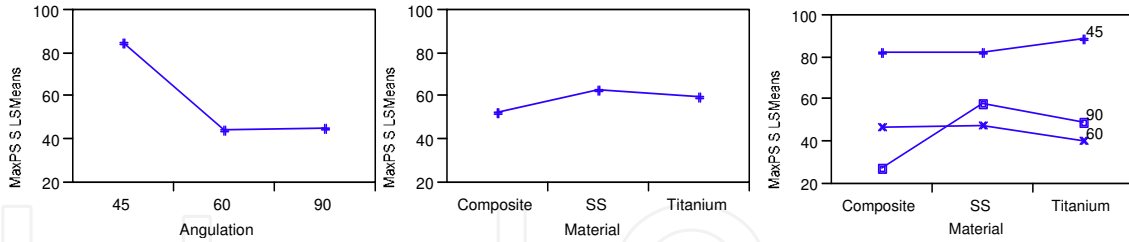
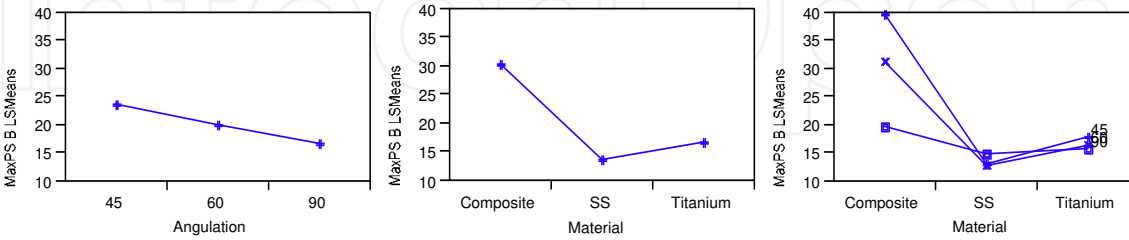


Fig. 7. Stress distributions of the orthodontic miniscrew showed that stresses concentrated in the neck region of the miniscrew at the interface between bone and the screw.

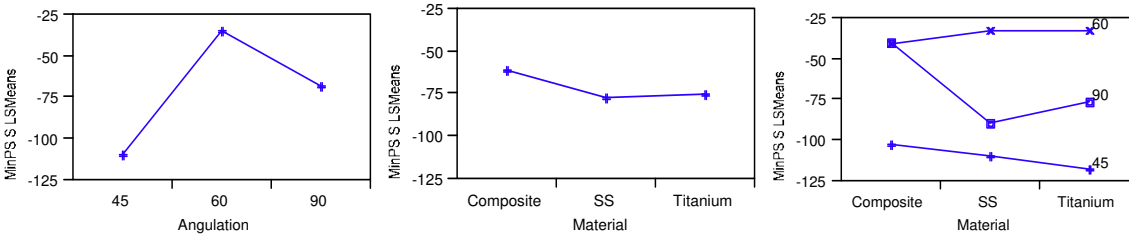
MaxPS S



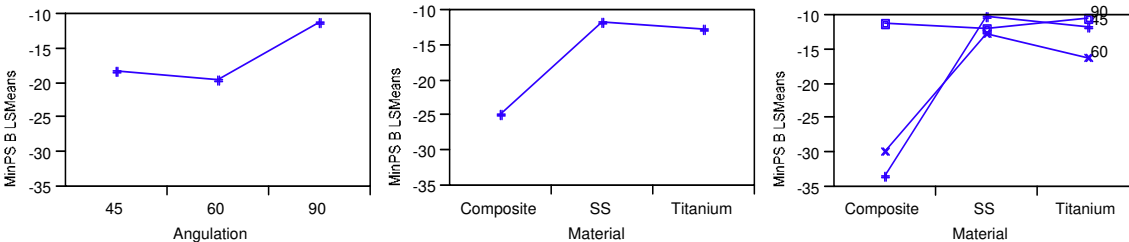
MaxPS B



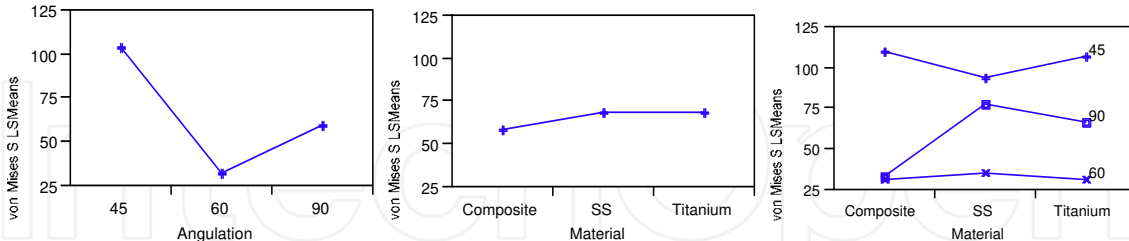
MinPS S



MinPS B



Von Mises S



Von Mises B

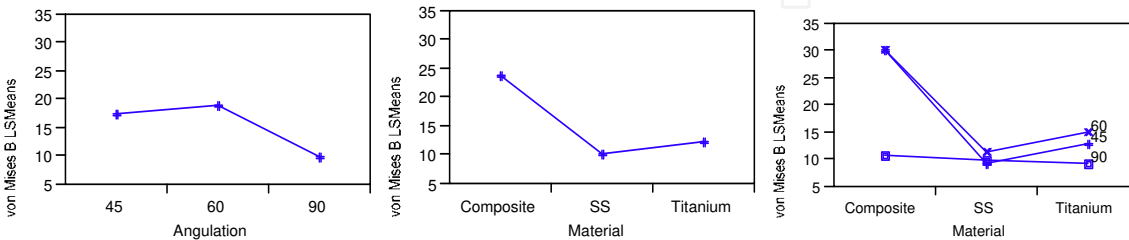


Fig. 8. Plots of mean stress (MPa) averaged over angulations (left column), materials (middle), and cross-action between angulation and materials (right). Symbols - MaxPS: maximum principal stress; MinPS: minimum principal stress; S: screw; B: Bone.

Angulation	Material	MaxPS		MinPS		vonMS	
		Mini-screw	Bone	Mini-screw	Bone	Mini-screw	Bone
45	Titanium	89.3	17.93	-117.63	-11.68	107.54	12.89
	Composite	82.99	39.94	-102.34	-33.26	110.09	30.33
	Stainless Steel	82.75	13.26	-109.24	-10.05	94.49	9.47
60	Titanium	40.31	16.55	-32.18	-16.23	31.56	15.13
	Composite	46.79	31.26	-40.29	-29.83	32.02	30.43
	Stainless Steel	47.53	12.74	-32.24	-12.62	35.35	11.42
90	Titanium	49.73	16.01	-75.82	-10.29	67.24	9.43
	Composite	27.91	19.81	-39.67	-11.25	33.55	10.99
	Stainless Steel	58.38	14.96	-88.9	-11.93	78.45	10

Table 2. Peak mean stress for each model.

Material effect

There is a noticeable ($p=0.05$) difference between material types with composite miniscrews having a higher average MaxPS and MinPS in cortical bone than Ti or SS. Peak MinPS is lowest on the miniscrew at 60° for Ti and SS miniscrews, and similar at 60° and 90° for composite. MinPS is greatest at 45° for all three materials. Peak MinPS is approximately the same in cortical bone for all three miniscrew materials at 90° (range -10.29 to -11.93 MPa) but at 45° and 60° MinPS in cortical bone is higher for composite than Ti or SS (-33.26 & -29.83 MPa respectively for composite vs. $-11.68/-10.05$ MPa & $-16.23/-12.62$ MPa for Ti/SS). When comparing the MinPS pattern generated for 45° , 60° , and 90° angulations, the composite miniscrew does not mimic the Ti or SS pattern. Rather, MinMS is substantially lower in both the miniscrew and bone at 90° than Ti or SS. Peak vonMS was lowest on the miniscrew at 60° for all three miniscrew materials relative to the other angulations. As with MinPS, the vonMS for the composite miniscrew differs from the Ti and SS pattern generated for 45° , 60° , and 90° angulations and is substantially lower in both miniscrew and bone at 90° than Ti or SS.

5.1.4 Discussion

One of the primary areas of interest in the present study related to the construction of a human model that is both realistic and of sufficient detail to clinically valuable. Comparing

these results to other orthodontic studies using FEA is challenging due to several differences between models. Many of the studies available in the literature do not model human anatomy (Gracco et al., 2009; Motoyoshi et al., 2005) and are not 3-dimensional (Brettin et al., 2008), or require additional resolution (Jones et al., 2001). Cattaneo et al (2009) produced a similar high-quality model of two teeth and surrounding bone for evaluation of orthodontic tooth movement and resulting periodontal stresses. Both linear and non-linear PDL mechanical properties were simulated. In a different study, Motoyoshi found peak bone vonMS in their model between 4-33MPa, similar to the levels in the current study (9.43-15.13MPa) However, Motoyoshi used a 2N (~203gm) force applied obliquely at 45°, different in both magnitude and orientation from that in this study.

From the results of the present study, an angulation of 60° is more favorable than either 45° or 90° for all three stress types generated relative to the stress on the miniscrew. Conversely, all three stress types have levels at 60° which are comparable to 45° and 90° in bone, so varied angulation within the range evaluated in the present study may not have a marked effect on the bone. However, miniscrews at 60° do have slightly higher MinPS (compressive) values than either 45° or 90°, which could have an effect on the rate or extent of biological activity and remodeling.

A third area of focus in the present study was the effect of using different miniscrew materials by comparing stress levels generated by popular titanium miniscrews with rarely- or never used stainless steel and composite miniscrews. Although no studies were found that compare Ti and/or SS miniscrews to composite miniscrews, one published study compared some of the mechanical properties of Ti and SS miniscrews (Carano et al., 2005). Carano et al reported that Ti and SS miniscrews could both safely be used as skeletal anchorage, and that Ti and SS miniscrew bending is >0.02mm at 1.471N (150gm) equivalent to the load applied in the present study. There was deformation of >0.01mm noted in the present study. However, the geometry in the study by Carano et al was otherwise not comparable to that in the present study.

There are no studies available which compare Ti and SS stresses or stress pattern generation. Therefore, to compare stresses generated from the use of composite to Ti and SS in the present study, the modulus of the miniscrew in each Ti model was varied to reflect that of SS and composite, with a subsequent test at each angulation. The fact that the general stress pattern for composite is dissimilar to Ti and SS when the miniscrew angulation is changed may be of clinical importance (Pollei 2009). Because composite has a much lower modulus than Ti or SS, it may be that stress shielding does not happen as much in composite miniscrews, and therefore more stress is transferred to the adjacent cortical bone in both compression and tension scenarios. As a result of increased compressive and tensile forces, especially in the 45° model, biological activity related to remodeling may be increased relative to other models with lower stress levels, and therefore have a more significant impact on long-term miniscrew stability and success. Another potential undesirable effect of using composite miniscrews in place of either Ti or SS is the increased deformation and distortion that is inherent due to the decreased modulus of composite relative to titanium or steel. Mechanical or design improvements need to be made to allow for composite miniscrews to be a viable alternative in clinical practice.

5.2 Orthodontic archwire

5.2.1 Introduction

Currently, biomechanical analysis of orthodontic force systems is typically limited to simple 2D force diagrams with only 2 or 3 teeth. Beyond this point, the system often becomes indeterminate. Recent laboratory developments (Badawi et al., 2009) allow investigation of the forces and moments generated with continuous archwires. However, this laboratory technique has 3 significant limitations: interbracket distance is roughly doubled, the PDL is ignored, and only a single resultant force and moment is calculated for each tooth.

The complete dentition CAD model assembled in our lab includes the PDL for each tooth and calculates the resultant stress-strain at any point in the model, improving on the limitations of the laboratory technique. However, the accuracy of this technique depends on the 3 factors mentioned previously: material properties, boundary conditions, and loading conditions. The considerations for material properties and boundary conditions are similar to the other models discussed above, but loading conditions with orthodontic archwires deserves closer attention.

Previously studies in orthodontics have typically used point-forces to load teeth, but fixed appliances rarely generate pure point-forces. In order to properly model a wide range of orthodontic movement, a new technique was developed which stores residual stresses during the insertion (loading) stage of the archwire, followed by a deactivation stage where the dentition is loaded equivalently to intraoral archwire loading. This method provides a new way to investigate orthodontic biomechanics (Canales 2011).

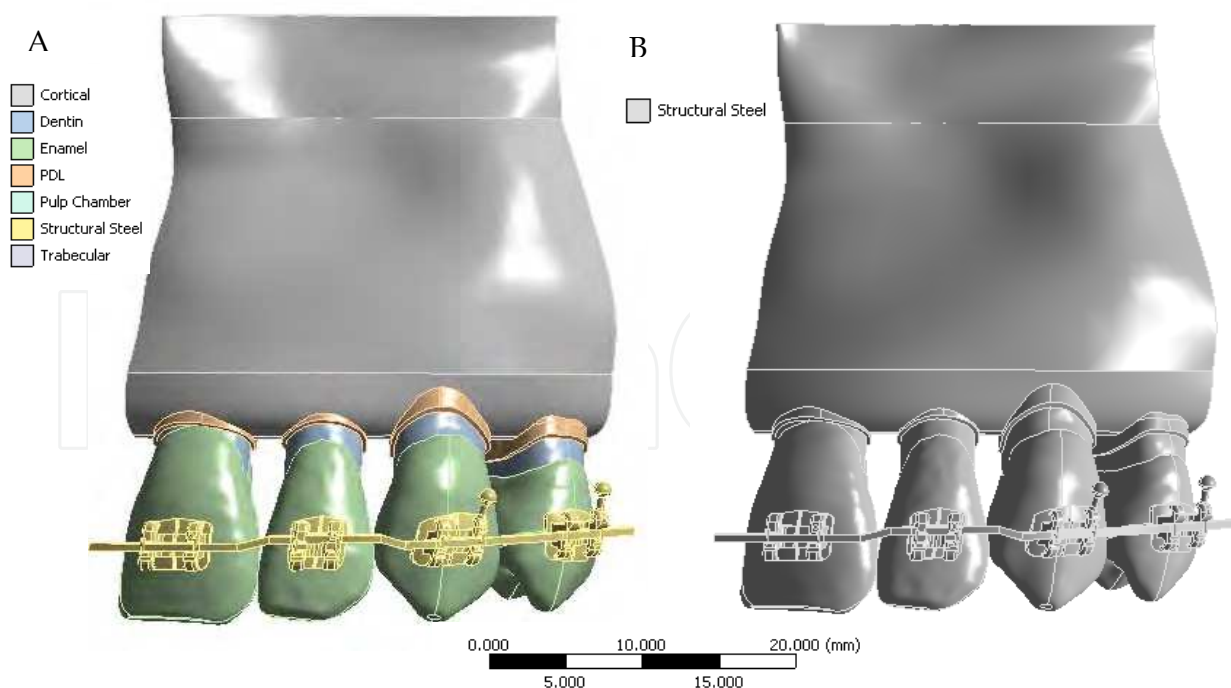


Fig. 9. Four tooth model used for FEA of continuous orthodontic archwires. A. Model with accurate material properties assigned to each body. B. Model with all bodies assumed to be stainless steel.

5.2.2 Methods

To assess the effect of proper PDL modeling, two separate models were generated from our master model. In both models, the upper right central incisor, lateral incisor, canine, and first premolar were segmented from the full model. Brackets (0.022" slot) were ideally placed on the facial surface of each tooth and an archwire was created that had a 0.5 mm intrusive step on the lateral incisor. Passive stainless steel ligatures were placed on each bracket keep the archwire seated. For one model, all bodies were assumed to be stainless steel (mimicking the laboratory setup by Badawi and Major 2009), while suitable material properties were assigned to each body in the second model (Figure 9). Each model was meshed using tetrahedral elements, except for swept hexahedral elements in the archwire, and consisted of 238758 nodes and 147747 elements. The ends of the archwire and the sectioned faces of bone were rigidly fixed. The contacts between the wire and the brackets were assumed frictionless.

5.2.3 Results and discussion

The static equilibrium equations were solved under large displacement assumptions. The final displacement in each model is shown in Figure 10, showing dramatically increased displacement in the PDL model. Notice that in both models, the lateral experienced unpredicted distal displacement due to the interaction of the archwire. This highlights the importance of accurate loading conditions in FEA. In addition to increased overall displacement, the center of rotation of the lateral incisor also moves apically and facially in the stainless steel model (Figure 11). Therefore, any results generated without properly modeling the PDL should be taken with caution - this includes laboratory testing of continuous archwire mechanics (Badawi and Major 2009).

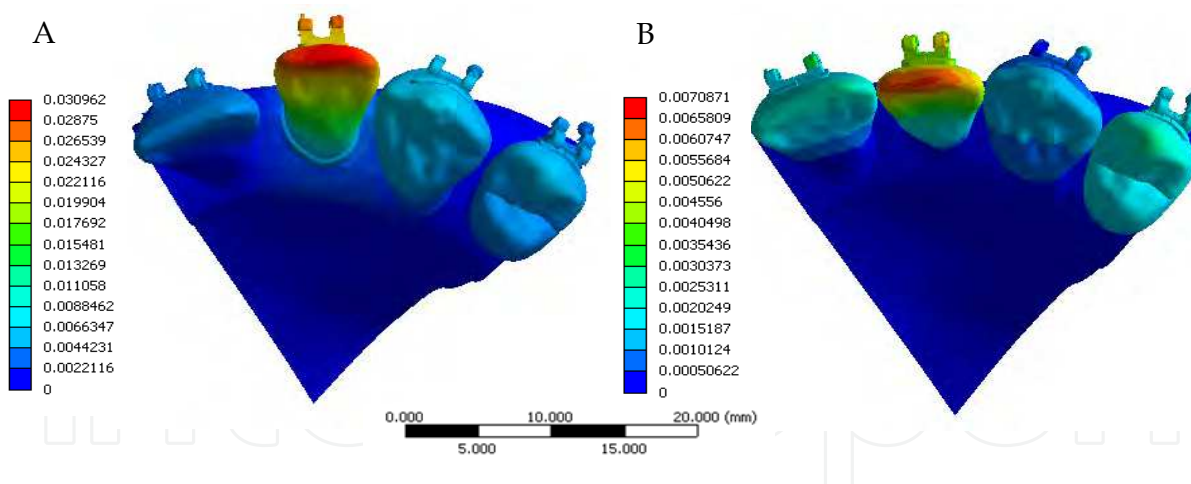


Fig. 10. Displacement viewed from the occlusal in the A) PDL model and B) stainless steel model after placement of a wire with 0.5 mm intrusive step bend. Note the different color scales and that both models have 7.1 times the actually displacement visually displayed.

The stress and strain distributions in the PDL also show variations in both magnitude and distribution (Figures 12 and 13). Unsurprisingly, the PDL shows increased strain when accurately modeled as a less stiff material than stainless steel. In this PDL model, the strain is also concentrated to the PDL, as opposed to more broadly distributed in the stainless steel model. Due to the increased rigidity in the stainless steel model, higher stresses were generated by the same displacement in the archwire.

The results clearly show the importance of the PDL in modeling orthodontic loading. We aim to further improve this model, adding additional teeth, active ligatures, and friction.

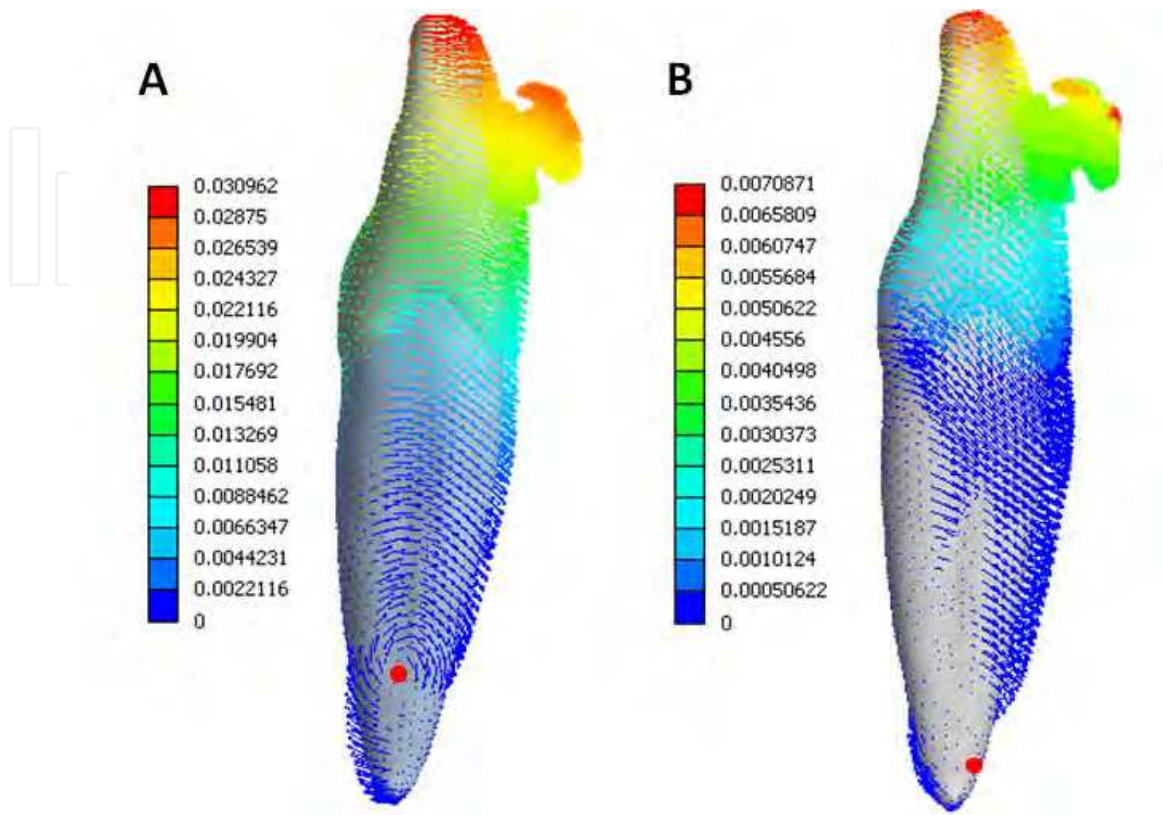


Fig. 11. Displacement viewed from the distal in the A) PDL model and B) stainless steel model after placement of a wire with 0.5 mm intrusive step bend. Note the center of rotation (red dot) in the stainless steel model moves apically and facially.

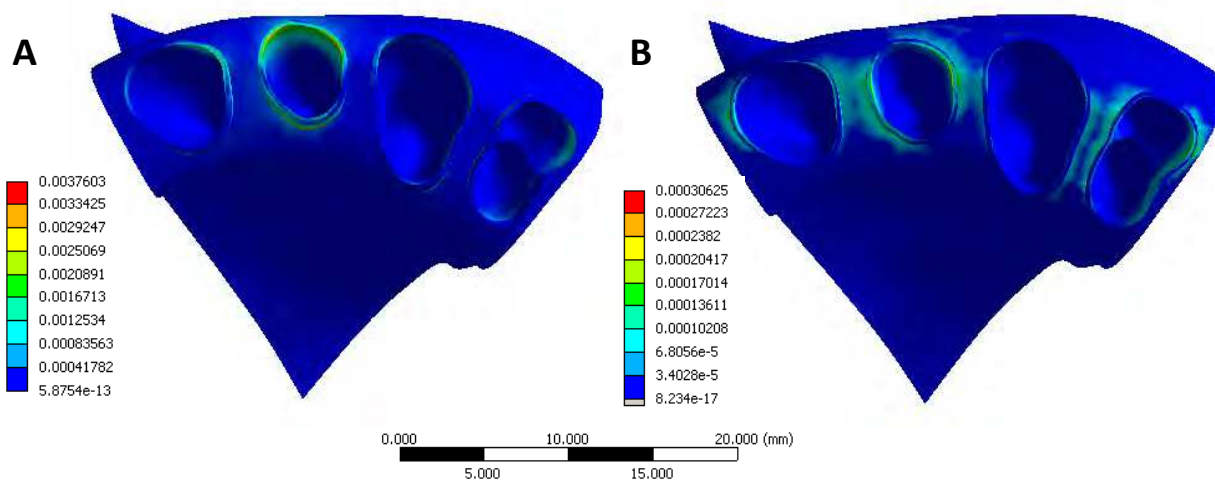


Fig. 12. Equivalent (von-Mises) elastic strain for the A) PDL model and B) stainless steel model after placement of a wire with 0.5 mm intrusive step bend.

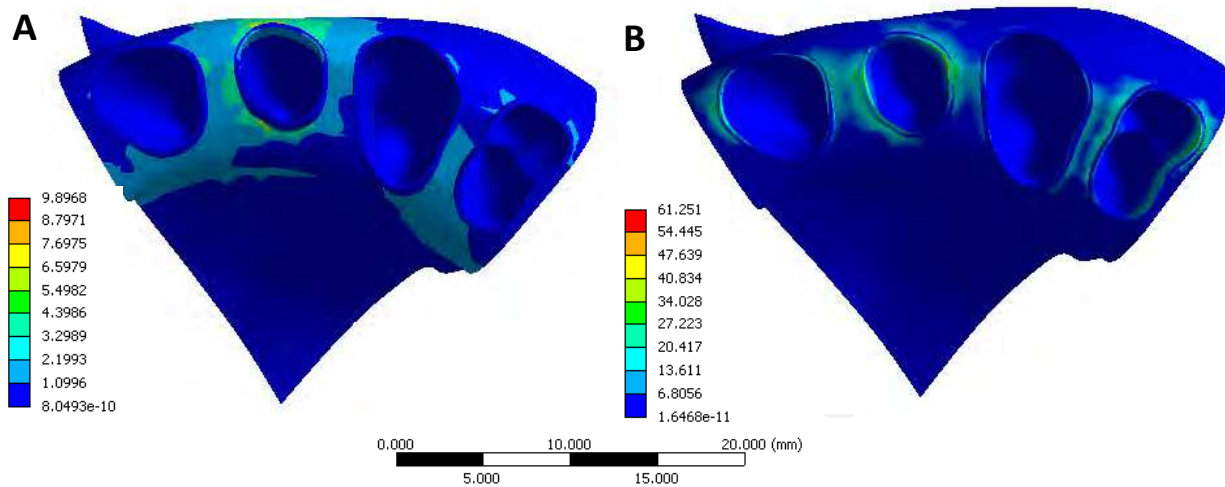


Fig. 13. Equivalent (von-Mises) stress in MPa for the A) PDL model and B) stainless steel model after placement of a wire with 0.5 mm intrusive step bend.

6. Future of dental FEA

Although FEA techniques have greatly improved over the past few decades, further developments remain. More robust solid models, like the one demonstrated in Figure 14, with increased capability to manipulate CAD objects would allow increased research in this area. The ability to fix minor problematic geometry and easily create models with minor variations would greatly reduce the time required to model different biomechanical

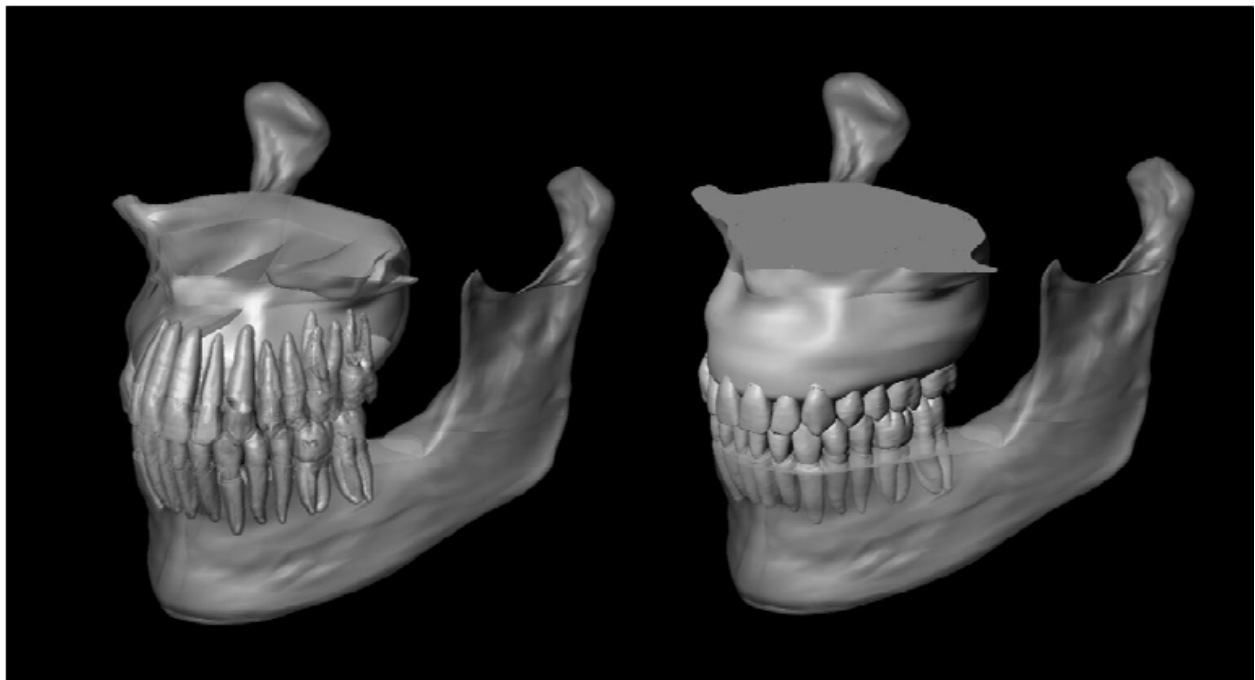


Fig. 14. Full Jaw Orthodontic Dentition (FJORD, UNC Copyright) Model: Isometric view of the solid models of mandible and maxillary arches and dentitions that was reconstructed and combined in SolidWorks software in our lab. The left image renders transparency of the gingiva and bone to reveal internal structures.

situations. Additionally, adding frictional boundaries conditions between teeth and active ligations for orthodontic appliances will continue to increase the accuracy of these models. Three dimensional dynamic simulations for assessing tooth injury, similar to those demonstrated in 2D studies (Huang et al., 2006; Miura and Maeda, 2008), should be re-evaluated. While techniques will continually be optimized to improve numerical approximations, this does not negate the value of finite element techniques in dentistry. These techniques use proven engineering principles to model aspects of dentistry that are unable to be efficiently investigated using clinical techniques, and will continue to provide valuable clinical insights regarding dental biomechanics.

7. Acknowledgement

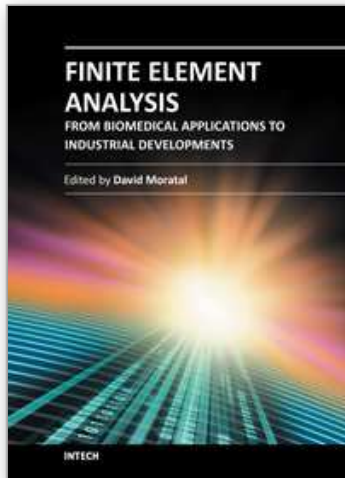
This study was supported, in part, by AAOF, NIH/NIDCR K08DE018695, NC Biotech Center, and UNC Research Council. We also like to thank Geomagic for providing software and technique supports to our studies.

8. References

- Anusavice KI, DeHoff PH, Fairhurst CW. Comparative evaluation of ceramic-metal bond tests using finite element stress analysis. 1980; *J Dent Res* 59:608-613.
- Badawi HM, Toogood RW, Carey JP, Heo G, Major PW. Three-dimensional orthodontic force measurements. *Am J Orthod Dentofacial Orthop.* 2009;136(4):518-28.
- Brettin BT, Grosland NM, Qian F, Southard KA, Stuntz TD, Morgan TA, et al. Bicortical vs monocortical orthodontic skeletal anchorage. *Am J Orthod Dentofacial Orthop.* 2008 Nov;134(5):625-35.
- Bright JA, Rayfield EJ. The response of cranial biomechanical finite element models to variations in mesh density. *Anat Rec (Hoboken).* 2011 Apr;294(4):610-20.
- Brosh T, Machol IH, Vardimon AD. Deformation/recovery cycle of the periodontal ligament in human teeth with single or dual contact points. *Archives of Oral Biology.* 2002; 47:85-92.
- Byrne DP, Lacroix D, Prendergast PJ. Simulation of fracture healing in the tibia: mechanoregulation of cell activity using a lattice modeling approach. *J Orthop Res.* 2011; 29:1496-1503.
- Canales CH. A novel biomechanical model assessing orthodontic, continuous archwire activation in incognito lingual braces. Master Thesis. University Of North Carolina-Chapel Hill. 2011.
- Carano A, Lonardo P, Velo S, Incorvati C. Mechanical properties of three different commercially available miniscrews for skeletal anchorage. *Prog Orthod.* 2005;6(1):82-97.
- Cattaneo PM, Dalstra M, Melsen B. Strains in periodontal ligament and alveolar bone associated with orthodontic tooth movement analyzed by finite element. *Orthod Craniofac Res.* 2009 May;12(2):120-8.
- Chi L, Cheng M, Hershey HG, Nguyen T, Ko CC. Biomechanical Re-evaluation of Orthodontic Asymmetric Headgear, In press. *Angle Orthodontist.* 2011. DOI: 10.2319/052911-357.1
- Farah JW and Craig RG. Distribution of stresses in porcelain-fused-to-metal and porcelain jacket crowns. *J Dent Res.* 1975; 54:225-261.

- Farah JW, Craig RG, Sikarskie DL. Photoelastic and finite element stress analysis of a restored axisymmetric first molar. *J Biomech.* 1973; 6(5):511-20.
- Field C, Ichim I, Swain MV, Chan E, Darendeliler MA, Li W, et al. Mechanical responses to orthodontic loading: a 3-dimensional finite element multi-tooth model. *Am J Orthod Dentofacial Orthop.* 2009;135:174-81.
- Geng J-P, Tan KBC, Liu G-R. Application of finite element analysis in implant dentistry: A review of the literature. *J Prosthet Dent* 2001; 85:585-98.
- Gracco A, Cirignaco A, Cozzani M, Boccaccio A, Pappalettere C, Vitale G. Numerical/experimental analysis of the stress field around miniscrews for orthodontic anchorage. *Eur J Orthod.* 2009 Feb;31(1):12-20.
- Hollister SJ, Ko CC, Kohn DH. Bone density around screw thread dental implants predicted using topology optimization, *Bioengineering Conference ASME BED* 1993; 24:339-342.
- Huang H-L, Chang C-H, Hsu J-T, Fallgatter AM, Ko CC. Comparisons of Implant Body Designs and Thread Designs of Dental Implants: A Three-Dimensional Finite Element Analysis. *The Int. J Oral & Maxillofac Implants.* 2007; 22: 551-562.
- Huang HM, Tsai CY, Lee HF et al. Damping effects on the response of maxillary incisor subjected to a traumatic impact force: A nonlinear finite element analysis. *J Dent* 2006;34:261-8.
- Hughes TJR. *The finite element method: linear static and dynamic finite element analysis.* Prentice-Hall, Inc. 1987.
- Huiskes R, Chao EYS. A survey of finite element analysis in orthopedic biomechanics: The first decade. *J. Biomechanics.* 1983; 6:385-409.
- Jones ML, Hickman J, Middleton J, Knox J, Volp C. A validated finite element method study of orthodontic tooth movement in the human subject. *J Orthodontics.* 2001; 28:29-38.
- Kim T, Suh J, Kim N, Lee M. Optimum conditions for parallel translation of maxillary anterior teeth under retraction force determined with the finite element method. *Am J Orthod Dentofacial Orthop.* 2010 May;137(5):639-47.
- Ko CC, Chu CS, Chung KH, Lee MC. Effects of posts on dentin stress distribution in pulpless teeth. *J Prosthet Dent* 1992; 68:421-427.
- Ko CC, Kohn DH, and Hollister SJ: Effective anisotropic elastic constants of bimaterial interphases: comparison between experimental and analytical techniques, *J. Mater. Science: Materials in Medicine.* 1996; 7: 109-117.
- Ko CC. Mechanical characteristics of implant/tissue interphases. PhD Thesis. University of Michigan, Ann Arbor. 1994.
- Ko CC. Stress analysis of pulpless tooth: effects of casting post on dentin stress distribution. Master Thesis. National Yang-Ming Medical University. 1989.
- Korioth TWP, Versluis A. Modeling the mechanical behavior of the jaws and their related structures by finite element analysis. *Crit Rev Oral Biol Med.* 1997; 8(1):90-104.
- Korioth TWP. Finite element modelling of human mandibular biomechanics (PhD thesis). Vancouver, BC, Canada: University of British Columbia. 1992.
- Lanczos C. *The variational principles of mechanics.* 2nd ed. University of Toronto Press. 1962.
- Liang W, Rong Q, Lin J, Xu B. Torque control of the maxillary incisors in lingual and labial orthodontics: a 3-dimensional finite element analysis. *Am J Orthod Dentofacial Orthop.* 2009 Mar;135(3):316-22

- Lin, C-L, Chang C-H, Ko CC. Multifactorial analysis of an MOD restored human premolar using auto-mesh finite element approach. *J. Oral Rehabilitation*. 2001; 28(6): 576-85.
- Magne P, Versluis A, Douglas WH. Effect of luting composite shrinkage and thermal loads on the stress distribution in porcelain laminate veneers. *J Prosthet Dent*. 1999 Mar; 81(3):335-44.
- Miura J, Maeda Y. Biomechanical model of incisor avulsion: a preliminary report. *Dent Traumatol* 2008;24:454-57
- Motoyoshi M, Yano S, Tsuruoka T, Shimizu N. Biomechanical effect of abutment on stability of orthodontic mini-implant. A finite element analysis. *Clin Oral Implants Res*. 2005 Aug;16(4):480-5.
- O'Brien, WJ. *Dental Materials and Their Selection* 2nd edition. Quintessence Publishing, 1997.
- Peter MCRB, Poort HW, Farah JW, Craig RG. Stress analysis of tooth restored with a post and core. 1983; 62(6):760-763.
- Pollei J. Finite element analysis of miniscrew placement in maxillary bone with varied angulation and material type. Master Thesis. University of North Carolina- Chapel Hill. 2009.
- Proffit WR, Fields HW, Nixon WL. Occlusal forces in normal and long face adults. *J Dent Res* 1983; 62:566-571.
- Proffit WR, Fields HW. Occlusal forces in normal and long face children. *J Dent Res* 1983; 62:571-574.
- Reinhardt RA, Krejci RF, Pao YC, Stannard JG. Dentin stress in post-reconstructed teeth with diminished bone support. *J Dent Res*. 1983; 62(9):1002-1008.
- Rieger MR, Mayberry M, Brose MO. Finite element analysis of six endosseous implants. *J Prosthetic Dentistry*. 1990; 63:671-676.
- Schmidt H, Alber T, Wehner T, Blakytyn R, Wilke HJ. Discretization error when using finite element models: analysis and evaluation of an underestimated problem. *J Biomech*. 2009; 42(12):1926-34.
- Seegerlind LJ. *Applied finite element analysis*. 2nd ed. John Wiley & Sons, Inc. 1984.
- Tanne K, Sakuda M, Burstone CJ. Three-dimensional finite element analysis for stress in the periodontal tissue by orthodontic forces. *Am J Orthod Dentofacial Orthop*. 1987; 92(6):499-505.
- Thresher RW and Saito GE. The stress analysis of human teeth. *J Biomech*. 1973; 6:443-449.
- Wang T, Ko CC, Cao Y, DeLong R, Huang CC, Douglas WH: Optical simulation of carious tooth by Monte Carlo method. *Proceedings of the Bioengineering Conference, ASME, BED* 1999; 42: 593-594.
- Yoshida N, Jost-Brinkmann PG, Miethke RR, Konig M, Yamada Y. An experimental evaluation of effects and side effects of asymmetric face-bows in the light of in vivo measurements of initial tooth movements. *Am J Orthod Dentofacial Orthop*. 1998; 113:558-566.
- Yushkevich PA, Piven J, Hazlett HC, Smith RG, Ho S, Gee JC, and Gerig G. User-guided 3D active contour segmentation of anatomical structures: Significantly improved efficiency and reliability. *Neuroimage*. 2006; 31(3):1116-28.
- Zienkiewicz OC, Kelly DW. Finite elements-A unified problem-solving and information transfer method. In: *Finite elements in biomechanics*. Gallagher RH, Simon. 1982.



Finite Element Analysis - From Biomedical Applications to Industrial Developments

Edited by Dr. David Moratal

ISBN 978-953-51-0474-2

Hard cover, 496 pages

Publisher InTech

Published online 30, March, 2012

Published in print edition March, 2012

Finite Element Analysis represents a numerical technique for finding approximate solutions to partial differential equations as well as integral equations, permitting the numerical analysis of complex structures based on their material properties. This book presents 20 different chapters in the application of Finite Elements, ranging from Biomedical Engineering to Manufacturing Industry and Industrial Developments. It has been written at a level suitable for use in a graduate course on applications of finite element modelling and analysis (mechanical, civil and biomedical engineering studies, for instance), without excluding its use by researchers or professional engineers interested in the field, seeking to gain a deeper understanding concerning Finite Element Analysis.

How to reference

In order to correctly reference this scholarly work, feel free to copy and paste the following:

Ching-Chang Ko, Eduardo Passos Rocha and Matt Larson (2012). Past, Present and Future of Finite Element Analysis in Dentistry, Finite Element Analysis - From Biomedical Applications to Industrial Developments, Dr. David Moratal (Ed.), ISBN: 978-953-51-0474-2, InTech, Available from:

<http://www.intechopen.com/books/finite-element-analysis-from-biomedical-applications-to-industrial-developments/past-present-and-future-of-finite-element-analysis-in-dentistry>

INTECH
open science | open minds

InTech Europe

University Campus STeP Ri
Slavka Krautzeka 83/A
51000 Rijeka, Croatia
Phone: +385 (51) 770 447
Fax: +385 (51) 686 166
www.intechopen.com

InTech China

Unit 405, Office Block, Hotel Equatorial Shanghai
No.65, Yan An Road (West), Shanghai, 200040, China
中国上海市延安西路65号上海国际贵都大饭店办公楼405单元
Phone: +86-21-62489820
Fax: +86-21-62489821

© 2012 The Author(s). Licensee IntechOpen. This is an open access article distributed under the terms of the [Creative Commons Attribution 3.0 License](#), which permits unrestricted use, distribution, and reproduction in any medium, provided the original work is properly cited.

IntechOpen

IntechOpen